Article

Not peer-reviewed version

Preparation and Characterization of Superabsorbent Polymers (SAPs) Based on PUL-g- AM/AA by Microwave Irradiation

Salam Abdulla Dhahir , Auda Jabbar Braihi , Salih Abbas Habeeb *

Posted Date: 29 May 2024

doi: 10.20944/preprints202405.1913.v1

Keywords: Superabsorbent polymers (SAPs); graft polymerization; hydrogels; microwave irradiation; pullulan

Article

Preparation and Characterization of Superabsorbent Polymers (SAPs) Based on PUL-g- AM/AA by Microwave Irradiation

Salam Abdulla Dhahir [1], Auda Jabbar Braihi [2] and Salih Abbas Habeeb [1,*]

Polymer and Petrochemical Eng. Dept. , College of Engineering Materials, University of Babylon, Iraq
* Correspondence: salihabbas014@gmail.com

Abstract: A microwave technique prepared a superabsorbent polymer (SAP) by grafting two hydrophilic monomers onto a polysaccharide substrate. The monomers used are acrylic acid (AA) or acrylamide (AM) to graft onto a pullulan substrate (PUL) to form PUL-g- AA (SAP1) and PUL-g- AM (SAP2), respectively. The monomers (AM/AA) graft together onto a PUL substrate to form PUL-g-(AM/AA) (SAP3). Grafting parameters such as grafting efficiency with percentage, conversion of monomer to polymer, gel content, water retention, water adsorption capacity, and swelling kinetics were determined. Additionally, the effect of environmental pH (2, 4, 7, 9, and 12) and sodium dodecylbenzene sulfonate (SDBS) surfactant was evaluated, where SDBS was added by 1,2,3,4 and 5 mM to form (SAP_4 to SAP_8). FTIR results show that AM grafted on PUL through an aliphatic C-N bond, while AA grafting occurred through a single C-C bond. The grafting efficiency with AM is higher than with AA, as well as their gel contents. Water absorbance capacity increased with grafting of AA or AM separately, and water retention was enhanced. The highest absorbent capacity, water retention, gel content and grafting parameters values were obtained with 3 mM SDBS content and pH7. The swelling kinetics showed that the increases in the theoretical and experimental swelling equilibriums were 72 % and 82%, respectively, at SAP_6 compared to the values of these parameters in SAP_3. The water absorption capacity of the hydrogel increases with increasing pH to 7 and then gradually decreases. XRD improves the crystallinity and crystalline size of the hydrogel after grafting polymerization for AM/AA into PUL, in addition to enhancing the thermal stability. On the contrary, FE-SEM demonstrated that SDBS improves the porosity and pore size of the hydrogel surface in SAP6.

Keywords: superabsorbent polymers (SAPs); graft polymerization; hydrogels; microwave irradiation; pullulan

1. Introduction

Super absorbent polymers (SAPs) contain large hydrophilic networks that allow them to absorb and retain large amounts of water or aqueous solutions, and it is difficult to remove the absorbed water with simple pressure [1]. These polymers have 3D networks that can absorb large amounts of water up to 300 times or more of their initial mass [2]. SAPs may be natural or synthetic depending on where they came from [3,4].

Ideal SAPs have high swelling capacity, rapid water absorption capacity, and high reusability [5]. The ability to absorb water by SAP depends on the hydrogen bonds with water molecules, the ionic concentration of the aqueous solution, and the type of bonds used to make the gel [6]. Polymers with a high ability to absorb are expressed as SAPs with low cross-linking density and lead to the formation of a softer gel [7]. Polymers with high-density cross-linked networks are characterized by low absorption and lead to the formation of a gel that is not flexible under the influence of simple pressure [8].

The biodegradability of natural SAPs such as cellulose, starch, and chitosan is a clear benefit. However, they are affected by the high amount of water required despite a low absorption rate [9,10].

 doi:10.20944/preprints202405.1913.v1

In contrast, despite the benefits of low cost, long service life, and high water absorption rate, the non-degradable characteristics of synthetic SAPs such as poly acrylic acid (PAA) and polyacrylamide (PAM) can have negative effects on the environment and plant growth [11,12]. There are many methods to improve the efficacy of SAPs, improve their hydrophilicity, and develop specialized network architectures, such as interpenetrating polymer networks (IPNs), semi-interpenetrating polymer networks (semi-IPNs), and copolymer networks [13]. Among many uses of SAP, they are used to manage the release of nutrients and to improve the efficiency with which soil uses water [5]. Therefore, the establishment of a porous structure is the key to enhancing swelling rate and regulating properties [8,14]. Currently, there are several technologies for the fabrication of porous hydrogels, including mainly freeze-drying [15], foaming [16], water-soluble boronogens [17], and the phase inversion technique [18].

Therefore, most of the above techniques are characterized by producing hydrogels with a large pore size distribution and closed pores [19,20]. Grafting polymerization is one of the important methods for the chemical modification of the polymers' specifications. Grafting methods include microwave radiation, plasma, ozone, and photometry [21]. The physical and chemical properties of polymers can be determined by polymerizing their surfaces using grafting, grafting from, or grafting through methods as a result of the good behavior of polymers after modifying their surfaces using graft polymerization [22]. Polysaccharides such as starch, cellulose, and chitin are polysaccharides that contain biomolecules and long-chain carbohydrates and several smaller monosaccharides [23].

Pullulan is a natural water-soluble polysaccharide with repeating units of malt triose residues extracted from the yeast-like fungus aureobasidium [24,25]. Due to its significant role in reducing ionic surface tension, sodium dodecylbenzene sulfonate (SDBS) is widely used in household detergents [26]. In addition, (SDBS) increases hydrogel surface porosity and swelling kinetics according to its concentration in superabsorbent polymers [27]. Microwave irradiation is frequently used in polymerization grafting reactions, especially when many monomers are grafted onto natural polymers, such as grafting acrylonitrile monomers onto guar gum, acrylamide onto chitosan and methyl methacrylate onto bamboo cellulose [28], in addition to the use of microwave radiation in the development of cross-linking in hydrogels and does not require a catalyst using high frequency electromagnetic waves [30]. Microwave irradiation has the advantages of low reaction time, increased production capacity, and high reaction control in terms of the least number of by-products and being environmentally friendly [31]. The microwave can provide the energy necessary to encourage the initiator to enter the reaction by overcoming the energies of some of its bonds, breaking them and forming free radicals, which represent active sites for starting the reaction [32].

This research aims to prepare super absorbent polymers (SAPs) using grafting polymerization (microwave irradiation) of acrylic acid and acrylamide monomers based on pullulan as substrate, and then compare the effects of SDBS surfactant and environmental pH from the viewpoint of swelling parameters.

2. Experimental Section

2.1. Materials and Methods

Pullulan (PUL) is used as a polysaccharide substrate, while acrylamide (AM) and acrylic acid (AA) monomers are used for grafting purposes. Sodium dodecylbenzenesulfonate (SDBS) (MW = 348 g / mol) is a surfactant. The chemicals needed to complete the research were purchased from Merck and used without further purification for the following purposes: Potassium persulfate (KPS) as an inorganic chemical reaction, was used as initiator, and N, N-methylene bisacrylamide (MBA) was used to form crosslinks. N, N-, N-tetramethylene diamine (TEMED) was used as an accelerator for the polymerization reactions while sodium hydroxide (NaOH) and solvents such as distaste water (DW), methanol, and ethanol were used for acid neutralization and washing, respectively.

 doi:10.20944/preprints202405.1913.v1

2.2. Preparation and Absorption Measurement of SAP

2.2.1. Preparation of SAPs

Superabsorbent polymers (SAPs) were made by grafting monomers (AM/AA) onto PUL according to the following steps:

1. Mixing monomers step: Mixing the AA and AM monomer solutions and adding MBA solution (0.04 g in 5 ml of DW). The AM monomer solution was prepared by dissolving 6 g in 12 ml of DW with continuous stirring. The AA solution was prepared in an ice bath to avoid polymerization by dissolving 6 g of AA monomer with partial neutralization (80% by weight) by 5 M NaOH.

2. Substrate preparation step: The Pullulan substrate was prepared by dissolving 1.20 g of PUL in 35 ml of distilled water about 3.2 wt. % concentration and mixing of the solution using a mechanical mixer at 60 ° C for 15 minutes, then adding aqueous solutions of SDBS surfactants with different concentrations (0, 1, 2, 3, 4 mM) with continuous mixing until a homogeneous solution is obtained.

3. Generation of free radicals: To facilitate the grafting step, free radicals were generated using a redox initiator system composed of two solutions: 0.118 g of KPS and 0.051 g of TEMED (each in 5 mL of DW). These solutions are added dropwise to the PUL solution at a temperature of 60 ° C for 10 minutes in the presence of high mechanical mixing.

4. Grafting step: The monomer solution (AM/AA) was added to the PUL solution after it was cooled to 50 ° C with mechanical mixing at a rotational speed of 1050 rpm for 15 minutes. The final solution of the reaction mixture was supplemented with 100 ml by adding DW, and the final solution was treated in a microwave oven at 475 watts for 4 minutes. The temperature and viscosity of the mixture gradually increased, and the gelation point was reached after 250 seconds; the product is a yellowish elastic gel. The SAP grafting polymerization reactions are explained in Figure 1.

5. Treatment of the final product: To remove the remaining surfactant, the resulting elastic gel was cut into small pieces and the resulting gel was washed several times with ethanol/water (10:1, v/v). Then the unreacted materials (PUL, AA, AM, KPS, TEMED, and MBA) were completely removed after immersion in pure methanol for 24 hours to dehydrate and dissolve without reacting. The final product was washed with ethanol, then ground and baked in an oven at 60 ° C for 24 hours [27,33].

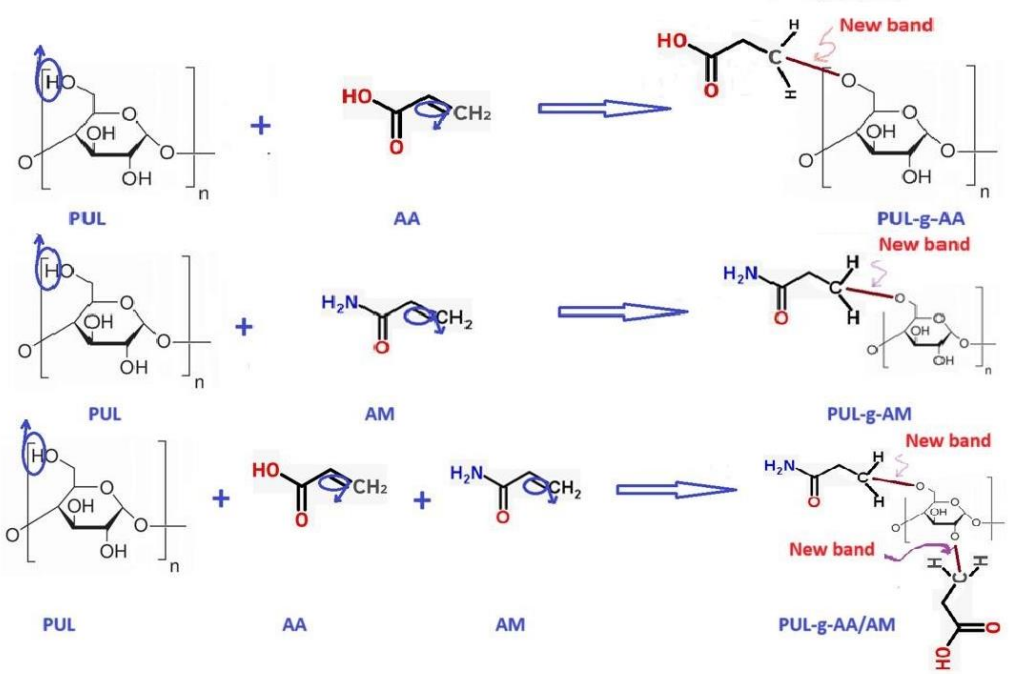

Figure 1. grafting polymerization reactions of SAP1, SAP2, and SAP3, respectively.

 doi:10.20944/preprints202405.1913.v1

2.2.2. Swelling Measurements

One hundred milligrams of SAP were immersed in 500 ml of distilled water at room temperature for 4 h until swelling was complete and a 150 µm sieve was used to filter the swollen gel. The sieve constantly is agitated to get rid of excess water until the water stops dripping from the sieve. The gel containing the absorbed water is weighed and the water absorption capacity of the gel is calculated according to the relationship [34,35]:

$$WAC = (W_s - W_d) / W_d \quad (1)$$

Where WAC is the water absorbency capacity, and (W_s,W_d) are the weights of swollen and dry specimens, respectively. The swelling kinetics was studied at different concentrations of SDBS (0, 1, 2, 3, and 4 mM) for several consecutive periods (1800, 3600, 5400, 7200, 9000, 10800, 12600, and 14400 seconds). Also, the effects of pH on swelling capacity were measured for aqueous solutions of various pH values (2, 4, 7, 9, and 12) at room temperature.

2.2.3. Measurement of Grafting Parameters

Gel Content: The gel content is measured by accurately weighing samples of the final product SAPs after polymerization. It is a dispersion of 0.1 g of the SAP sample prepared in distilled water (DW) until complete swelling is reached, then it is filtered through a sieve and washed with distilled water several times. The samples are dehydrated in excess ethanol for 48 hours and dried at 50 ° C for 12 hours until the SAPs have a constant weight. It is calculated according to the following relationship [36]:

$$Gel(\%) = (W_d/W_i) * 100 \quad (2)$$

WhereW_d, W_i are the weight of dried hydrogel after extraction and the initial weights of SAPs, respectively?

Grafting Polymerization: the weight percentage of synthetic polymer branches grafted onto functional groups of the pullulan to the total synthetic polymer, including grafted branches and ungrafted photopolymers. Grafting percentage (G (%)), Grafting efficiency ($E(\%)$), and Conversion of monomers to polymers (C (%)) are determined by the following relations [37]:

$$G(\%) = \frac{W1}{W2} * 100 \quad (3)$$

$$E(\%) = \frac{W3}{W4} *100 \quad (4)$$

$$C(\%) = \frac{W1}{W5} *100 \quad (5)$$

where W1, W2, W3, W4 and W5 are the weight of monomers in a grafted polymer, the weight of the polymer taken, the weight of the grafted polymer, the weight of (polymer and monomers) taken, and the weight of monomers taken.

Water retention: The swollen pre weighed and water-equilibrated gel (Weq) is placed in distilled water for 24 hours at room temperature. The weight of hydrogels (Why) is weighed, and water retention is calculated according to the following relationship: [38]:

$$WR(\%) = \left(W_{hy}/W_{eq}\right) * 100 \quad (6)$$

Where Weq and Why are the swollen pr-weighed and water-equilibrated gels and the weights of hydrogels, respectively.

 doi:10.20944/preprints202405.1913.v1

2.3. Characterization

The FTIR test was carried out to identify the chemical structure of PUL, AA, and AM, where the IR spectra recorded in the range of 400–4000 cm^{-1} were recorded. This technique also proposes the grafting model (if any) among these components.

In the XRD technique (D8 Bruker, Germany), data was collected at 0.02-degree intervals with a count of 0.5 s per step in the 2 ° range of 10–80 °. This test was achieved to monitor the effects of surfactant concentrations on crystallite size and crystallinity percentage. The DSC-TGA technique (SDT Q600 V20.9 Build 20) was used to study thermal transitions and thermal stability. On the contrary, the morphological properties of the samples' surfaces were studied using the FE-SEM technique (ZEISS Sigma) .

3. Results and Discussions

3.1. Prepared SAPs

A group of SAP based on PUL has been prepared according to the composition details mentioned in Table 1, such as (SAP_1): PUL-g- AA; (SAP_2): PUL-g- AM; (SAP_3): PUL-g- AM/AA; (SAP_6): PUL-g- AM/AA - 3 mM SDBS, respectively.

Figure 2A shows the FE-SEM images of various SAPs, the weak bond between the SAP_1 and ASP_2 gel particles, a three-dimensional network connecting the gel particles at SAP_3 and SAP_6 and the formation of pores due to the interlocking structures of the hydrogels shown in the PUL-g-AM/AA structure. The SDBS surfactant altered the compact structure of PUL-g-AM / AA to a rough surface with deep pores in the hydrogel surface, which means that SDBS acts as a pore-forming agent; these pores become clearer after washing the hydrogel with ethanol (Figure 2B). This is due to the self-assembly of SDBS particles in the reaction medium. Microwave provides the energy needed to activate the initiator (KPS) to generate free radicals and accelerate the polymerization reaction using the (TEMED) [65]. The radicals start the grafting reaction in vinyl monomers such as AA and AM in the double bond of C=C and then propagate to the polymeric chain [39]. The results of FE-SEM coincide with the proposed models; As the graft increased (such as in SAP_3), the surface became rougher and contained more porous, which makes it capable of absorption of more amounts of water.

Table 1. Composition of samples of the prepared SAPs.

Samples	Composition of SAPs
SAP_1	PUL-g- AA
SAP_2	PUL-g- AM
SAP_3	PUL-g- AM/AA
SAP_4	PUL-g-AM/AA - 1 mM SDBS
SAP_5	PUL-g- AM/AA - 2 mM SDBS
SAP_6	PUL-g- AM/AA - 3 mM SDBS
SAP_7	PUL-g- AM/AA - 4 mM SDBS
SAP_8	PUL-g- AM/AA - 5 mM SDBS

Preprints.org (www.preprints.org) | NOT PEER-REVIEWED | Posted: 29 May 2024 doi:10.20944/preprints202405.1913.v1

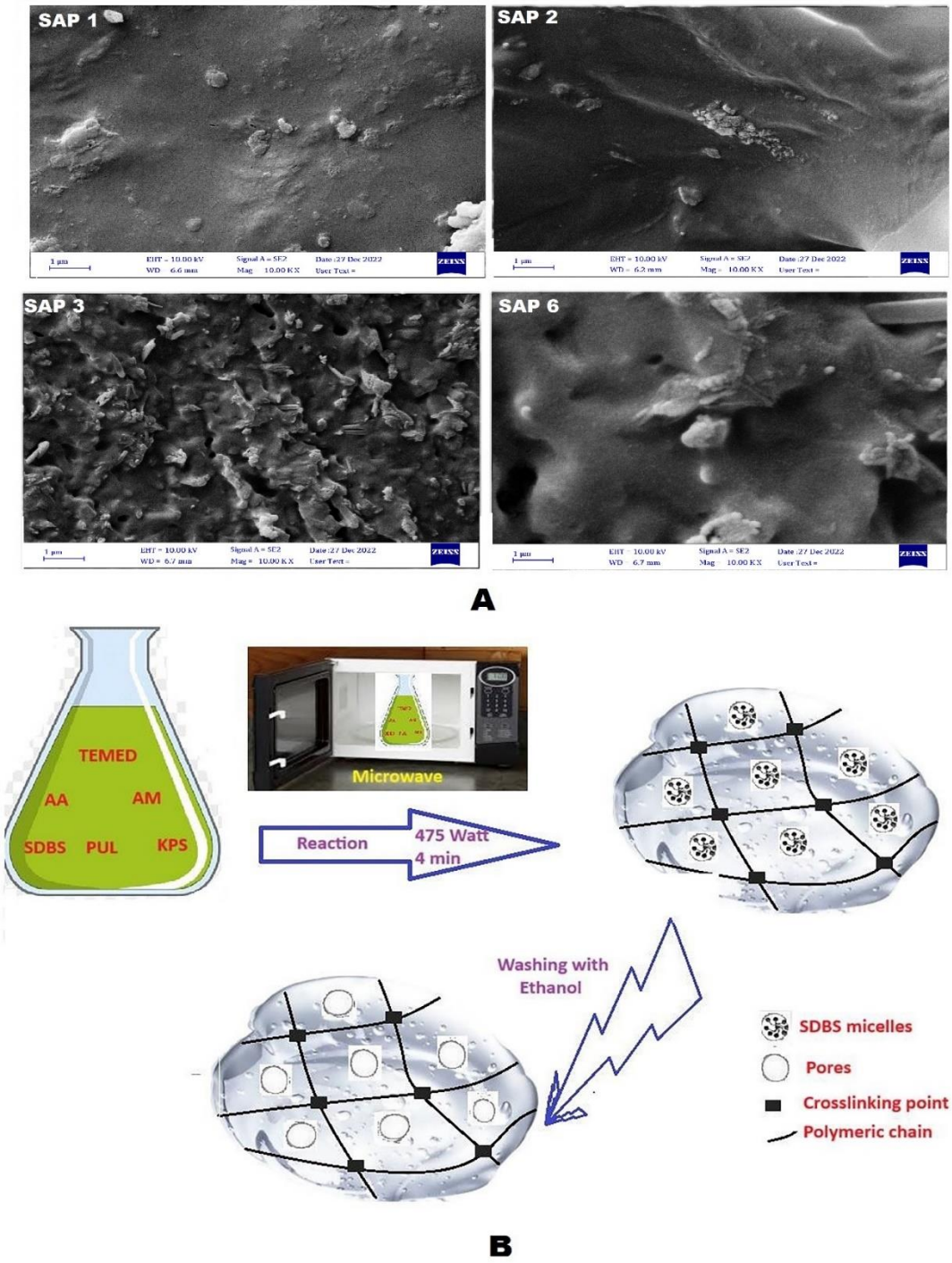

Figure 2. (A) 1 μm of FE-SEM images for SAP_1, SAP_2, SAP3 and SAP6, respectively; (B) Schematic of the formation of the SDBS micelle template during the reaction and after washing with ethanol.

The (FE-SEM) as shown in Figure 1, determined the morphological properties of the hydrogels, such as pore volume (nm^3) and porosity (%), which were measured by ImageJ software. The porosity of the hydrogels can be calculated by comparing the average pore volume with the volume of the FE-SEM image using the following equation [40]:

$$\text{Porosity (\%)} = \frac{V_p}{V_{total}} * 100 \quad (7)$$

 doi:10.20944/preprints202405.1913.v1

According to equation 6, the porosity % increased with an increase in the pore volume of the hydrogel. The percentage of increment in the pore volume was 263.78 % after adding 3 mM SDBS to the PUL-g-AM /AA; the results of pore volume (nm ^{3}) and porosity % of SAPs are shown in Table 2. The pore volume of the hydrogel increased with SDBS compared to the pore volume of the hydrogel that did not contain SDBS [41].

Table 2. Results of pore volume (μm ^{3}) and porosity % of SAPs.

Samples	Pore volume (nm ^{3})	Porosity %
SAP1	22.53±11.34	5.318
SAP2	32.85±10.30	9.223
SAP3	62.56±10.17	11.822
SAP6	227.58±8.183	15.903

3.2. FTIR Analysis

FTIR spectroscopy was used to specify the chemical composition of each component and to determine whether there is a chemical reaction between these components. Figure 3 shows the FTIR spectra of PUL, PUL–g- AA, PUL-g- AM and PUL-g-AM/AA. For the PUL spectrum (Figure 3A), bands from 738-to 933 cm^{-1} belong to α-(1, 4) and α-(1, 6) -D-glucosidic bonds. Bands at 1148 cm^{-1} and 1373 cm^{-1} are due to the C-O-C and C-O-H, respectively, while band 1636 cm^{-1} is due to the stretching vibration of the O-C-O group. A band at 2924 cm^{-1} is due to SP^3 of the C-H bond, while O-H stretching vibration occurred from 3217 cm^{-1} to 3420 cm^{-1} [42]. For the acrylic acid spectrum (Figure 3B) spectrum, the band at 3417 cm^{-1} belongs to the O-H stretching vibration mode. A band at 2924 cm^{-1} is due to the stretching vibration of CH in the methylene group. The carbonyl group (C=O) appears at 1634 cm$^{-1,}$ and the bending vibration of the CH2 group occurred at 1440 cm^{-1}. The bending of the O-H group happened at 1381 cm^{-1}, while the C-C stretching occurred at 1161 cm^{-1} and the C-OH stretching at 1026 cm^{-1}; the out-of-plane vibration mode for =CH and =CH_2 occurred at 871 cm^{-1} and 810 cm^{-1} respectively [39].

For the Acrylamide spectrum (Figure 3C) spectrum, bands from 3240 cm^{-1} to 3418 cm^{-1} belong to the symmetrical and asymmetrical stretching vibrations of the N-H group. In contrast, the band at 2932 cm^{-1} belongs to the stretching vibration of the methylene (CH_2) group. The bending vibration of the N-H group appears at 1582 cm^{-1}, while the symmetrical stretching vibration of the carbonyl group (C=O) appears at 1620 cm^{-1}.

Preprints.org (www.preprints.org) | NOT PEER-REVIEWED | Posted: 29 May 2024 doi:10.20944/preprints202405.1913.v1

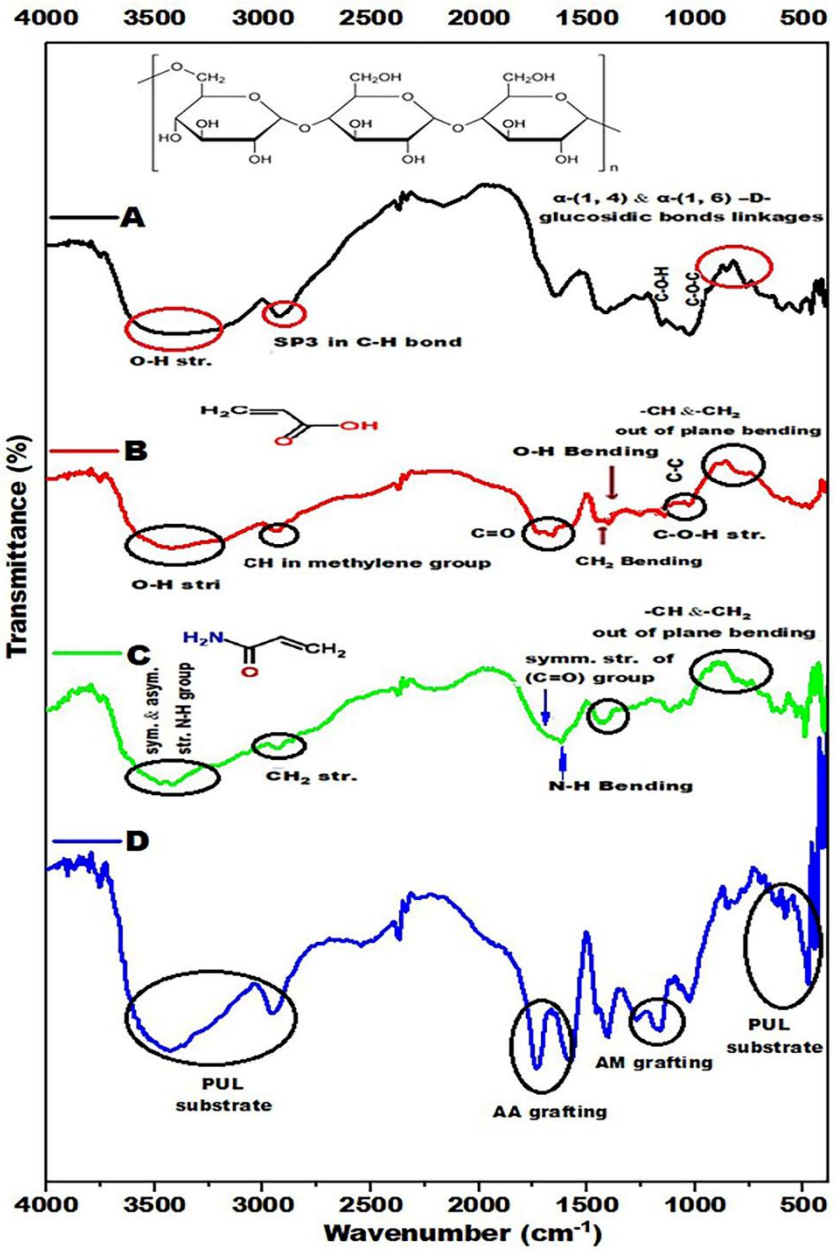

Figure 3. FTIR analysis of (A) PUL,(B) PUL-g- AA, (C) PUL-g- AM, and (D) PUL-g-AM/AA after washing.

At 1404 $cm^{-1,}$ the bending vibration of the CH_2 group occurred, while the bending out of the plane of = CH and $–CH_2$ occurred at 779 cm^{-1} and 849 $cm^{-1,}$ respectively [43]. It is clear from Figure 3D that all three components are present in the structure of the polymeric blend. The appearance of bands from about 1600 -1700 cm^{-1} indicates AA grafting, where AA contains a carboxyl group (COOH) [39]. This group includes the OH and C=O groups, which usually appear at these positions. The AM grafting appearance at the bands about 1000-1250 cm^{-1} and PUL substrate appearance at bands about 3000-3600 cm^{-1} and 450-750$cm^{-1,}$ respectively.

The AM was grafted onto the PUL substrate through an aliphatic C-N bond, where its band appeared at 1000 - 1250 cm^{-1}. In contrast, AA grafting occurred through a single C-C bond, but since this bond is nonpolar (no difference in electronegativity), it usually does not show up as peaks in the IR spectrum. A covalent bond consists of two electrons from each of two carbon atoms. It is called a sigma bond (σ) between one orbital of each carbon atom.

 doi:10.20944/preprints202405.1913.v1

3.3. XRD Analysis

The X-ray diffraction patterns of SAP_1, SAP_2, SAP_3, and SAP_6 with a range of 10- 80° and the results of the crystalline properties as shown in Figure 4 and Table 3. The peaks of the board peaks of all samples with 2θ = 18.775-21.94°. The grafting reaction among the PUL, PAA, and PAM monomers altered the crystalline structure, where the crystallinity percent obtained and the crystallite size of the final structure were in between its values for the two monomers in the orthogonal planes of the Miller indices (h k l) (110) according to the d spacing of 3.569 and 4.115 for SAP1 and SAP2. However, the orthogonal planes of the structure change to (220) with a spacing of 2.378 Å when grafting two monomers AM / AA on the PUL substrate at 2θ= 49.825, also changing the orthogonal planes of the Miller indices (h k l) to (211) after adding SDBS to the hydrogel reaction. Generally, PUL-g-AM / AA with and without SDBS has a partially crystalline hydrogel structure due to the formation of intramolecular hydrogen bonds between the polymer chains in the internal hydrogen structure [27,44,45].

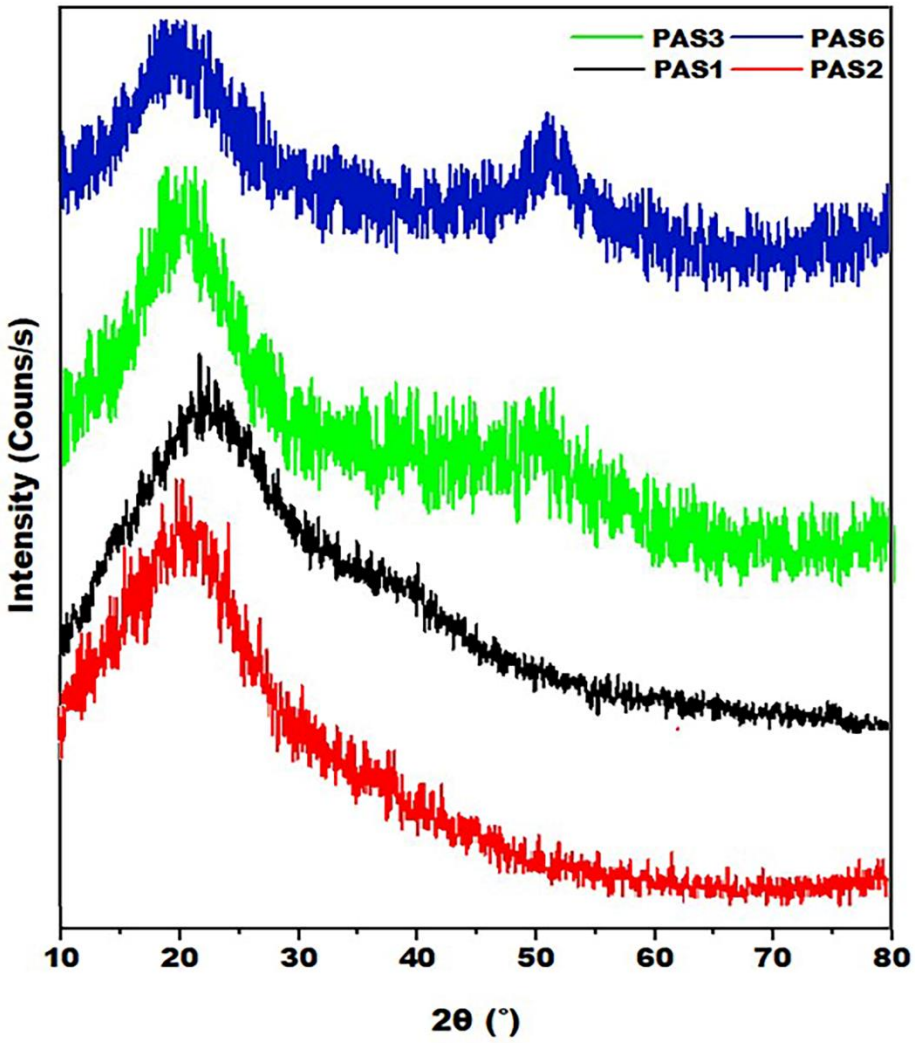

Figure 4. XRD patterns of SAP_1, SAP_2, SAP3, and SAP6, respectively.

Table 3. Crystallinity percent and average crystalline size of some prepared SAP.

SAPs	Pos. [°2Th.]	d-spacing [Å]	FWHM [°2Th.]	(h k l)	Crystallinity (%)	Crystallite Size (nm)
SAP_1	21.59	3.569	0.16593	110	15.02	48.46
SAP_2	21.94	4.115	0.15884	110	11. 35	40.86

 doi:10.20944/preprints202405.1913.v1

SAP_3	18.78	4.725	0.35080	110	22.61	51.60
	49.83	2.378	0.16320	220		
SAP_6	19.73	3.335	0.17640	110	23.87	54.30
	50.43	1.809	0.16211	211		

(h k l): Miller indices.

3.4. Thermal Properties

Figure 5 shows the DSC curve (red) and the TGA curve (black) for the prepared SAP, while Table 4 summarizes the weight loss steps for heated samples up to 800 ° C. The results showed that the thermal stability of SAP_1 is better than that of SAP2, as it is almost uniform, while in the SAP2 sample, it is irregular, and the sample loses 63.4% of its weight at 300 ° C. On the other hand, grafting each of AA and AM on PUL enhances resistance to thermal decomposition. However, the addition of SDBS works strongly to enhance the thermal behavior of the SAP6 sample, as there is no loss of weight in the sample at 220 ° C compared to all samples, and the thermal decomposition is uniform according to the weight loss steps compared to the SAP3 sample, which lost almost half of its weight at 800 ° C. The influence of SDBS surfactant on the thermal stability and thermal transitions of PUL- g- AM/AA, the weight loss up to 800 ° C is 86.46% (SAP_3), while this loss decreased to 72.59 % for a sample with 3 wt. % SDBS (SAP_6) at 800 ° C. It was also noted that weight loss occurred gradually and less severely than in the SDBS-free sample. This indicates that SDBS enhances the stability of the hydrogel [46]. Temperature over time. Generally, the first step for SAPs represented the elimination of adsorbed-free water, and the second step represented the dehydration of the saccharide rings and depolymerization with the formation of water, CO2, and CH4 [47].

Table 4. Weight loss results of SAP samples according to many degradation steps.

SAPs	Tw	Step -1		Step -2		Step -3		Step -4		Step -5	
	(%)	A	B	A	B	A	B	A	B	A	B
SAP_1	81.78	150	1.88	220	8.38	370	14.7	480	35.00	800	21.82
SAP_2	90.92	125	4.23	300	53.53	470	22.2	800	10.96	-	-
SAP_3	86.46	150	1.56	370	42.60	800	42.3	-	-	-	-
SAP_6	72.59	220	none	260	5.03	370	23.5	470	18.20	800	25.86

A: Temperature (°C); B: Weight loss (%); Tw: Total weight lost (%).

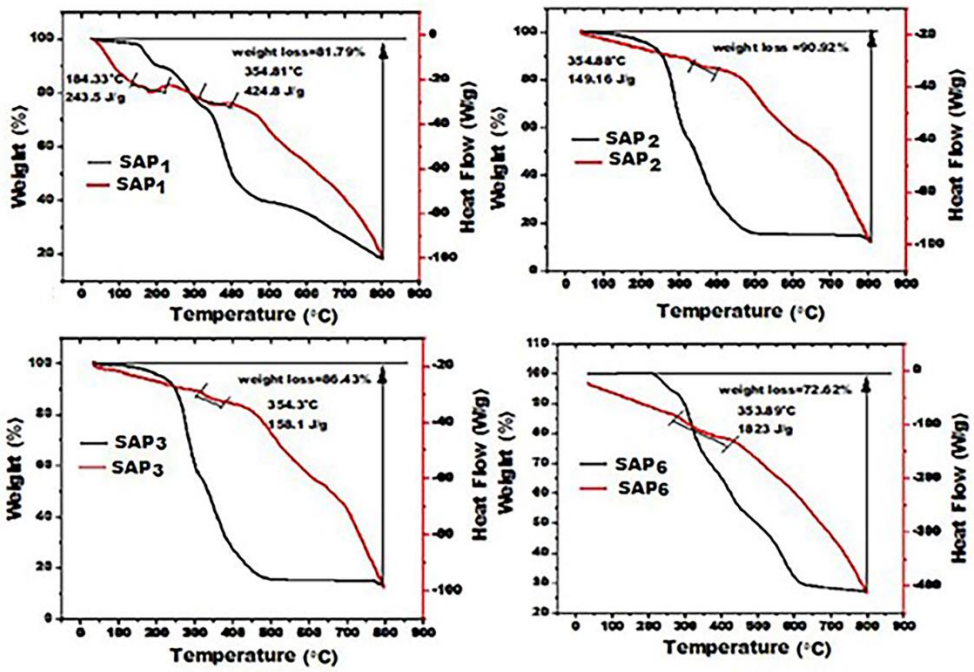

 doi:10.20944/preprints202405.1913.v1

Figure 5. DSC-TGA curves for SAP_1, SAP_2, SAP3 and SAP6, respectively. .

This is because SDBS, during polymerization, promotes the emulsification of droplets of the AA and AM monomers, resulting in the solubilization of these two monomers within the micelles and increasing the number of nucleated particles [48]. This behavior is expected to increase the crystallinity degree. The same finding can be concluded from the DSC curve, where the enthalpy of the thermal transition increased from 158.1 J / g in SAP_1 to 1823 J / g in SAP_6. The previous results coincide with the increase in crystallinity (%) and crystallite size obtained from the XRD test.

3.5. Effect of SDBS on the Absorption and Grafting Parameters

For the prepared samples, many absorptions and grafting parameters were calculated, such as water retention (WR), gel content (Gel), percentage of grafting (G), grafting efficiency (E), and water absorption capacity (WAC), as shown in Table 5.

The effects of SDBS concentrations on these properties have a considerable dependence on the concentration of the surfactant in the samples (SAP_3 to SAP_8) compared to the variation of these parameters without SDBS and the grafting used only AA or AM monomers in PUL as (SAP_1 and SAP_2) [39], indicating that micelle creation encourages both swelling and grafting processes. It can be noted that the percentage of water retention in the presence of SDBS increases to 60% compared to 20% for the hydrogel without SDBS. Furthermore, Gel (%), G (%) and E (%) are the highest at SAP_6 (PUL-g- AM/AA- 3 mM SDBS). This means that there is an optimal concentration of the surfactant. Beyond it, the pore-forming ability of SDBS becomes invalid [27,49]. These results agreed with the results of the previous study [27].

Table 5. Absorbance and grafting parameters for the prepared samples at room temperature and 7 pH.

Sample	C (%)	G (%)	E (%)	Gel (%)	WAC (g/g)	WR (g/g)
SAP_1	72.07	325.0	65.00	51.70	32.0	63.70
SAP_2	73.19	333.3	66.67	61.80	58.0	68.00
SAP_3	83.57	743.3	74.33	73.00	74.1	73.44
SAP_4	87.03	760.0	76.00	74.39	123.5	74.93
SAP_5	88.32	783.3	78.33	78.72	143.6	76.00
SAP_6	89.95	838.3	83.83	81.40	200.5	79.50
SAP_7	89.13	820.0	82.00	74.81	137.8	73.09
SAP_8	88.86	800.0	80.00	78.88	128.7	71.54

C.: Conversion of monomer to polymer G: Grafting Percentage; E: Grafting Efficiency; Gel: Gel Content; WA: Water Absorbent Capacity; WR: Water Retention.

3.6. Effect of SDBS on Absorption Capacity and Swelling Kinetics

Research studies have shown that hydrogel porosity plays an important role in increasing water absorption, and this property has increased the agricultural applications of this type of polymer [50]. Based on the morphological properties, which were confirmed by the FE-SEM images and the results of the adsorption parameters (water absorbent capacity) in Table 4 and Figure 6 show the increase in the amount of water absorbed by the prepared SAP with the increase in the absorption time to reach the equilibrium limit as a function of the concentration of SDBS. Reaching the equilibrium state means that both expansion due to penetration through osmotic pressure by the solvent or contraction led to a decrease in enthalpy and the formation of the elastic strength of the network [51].

Figure 6 and Table 6 show the effect of surfactant concentrations on the swelling (S_w) of the samples prepared. The results showed that the highest absorbance of water swelling absorbance (S_w) was obtained with the 3 mM SDBS content. The hydrogel structure was more porous, and the larger

Preprints.org (www.preprints.org) | NOT PEER-REVIEWED | Posted: 29 May 2024 doi:10.20944/preprints202405.1913.v1

the specific surface area, the faster the water diffusion into this structure. Hydrogel porosity is one of the most important factors affecting the absorption of these polymers [14].

From the kinetic point of view of swelling, it is clear that swelling gradually increased with time, then was stable at the final stage where the equilibrium state occurred.

The Schott second-order swelling kinetic model was proposed to study the absorption kinetic. The relation between the average swelling rate (t / S_w) and swelling time (t) gives straight lines according to the proposed model [42]:

$$t/S_{w=} = 1/K_{it} + 1/S_{\infty}\, t \qquad (8)$$

Where S_w is the swelling ratio at time$t$, $S_{\infty}$is the theoretical equilibrium swelling ratio, which is the slopes of these lines, and K_{it} is the initial swelling rate constant, which is equal to the intercept of the fitted straight lines with the Y axis.

Table 5 also showed that both $S_{\infty}, and\ S_{eq}$ have the same manner, where their maximum values were obtained with the 3 mM SDBS content. The theoretical values of the equilibrium swelling ratio S_{∞} values are consistent with the equilibrium water absorption S_{eq} and increase with increasing SDBS concentration up to 3 mM concentration. The initial swelling rate constant K_{it} values change with SDBS concentration change, and the highest value at 3 mM concentration in addition to the rate correction factor is $R^2 > 0.98$, indicating the precision of the results.

Table 6. The comparison between Schott's pseudo-second-order swelling kinetics model results from the effect of SDBS concentration and changing pH values.

	Swelling Kinetics Parameters					Swelling Kinetics Parameters			
SBDS (mM)	R^2	K_{it}	S_{∞}	S_{eq}	**pH**	R^2	K_{it}	S_{∞}	S_{eq}
0	0.935	0.017	95.69	74.1	2	0.987	0.054	123.00	110.2
1	0.987	0.051	140.65	123.6	4	0.986	0.073	123.30	116.7
2	0.993	0.077	151.52	137.8	7	0.994	0.146	211.86	200.5
3	0.997	0.150	213.68	200.5	9	0.985	0.074	130.55	122.0
4	0.997	0.106	153.37	142.6	11	0.982	0.065	72	121.9
5	0.998	0.123	135.50	128.6					

R^2: Correction factor; K_{it} Initial swelling rate constant; S_{∞}: Theoretical equilibrium swelling; S_{eq}: stabilized equilibrium absorbency

 doi:10.20944/preprints202405.1913.v1

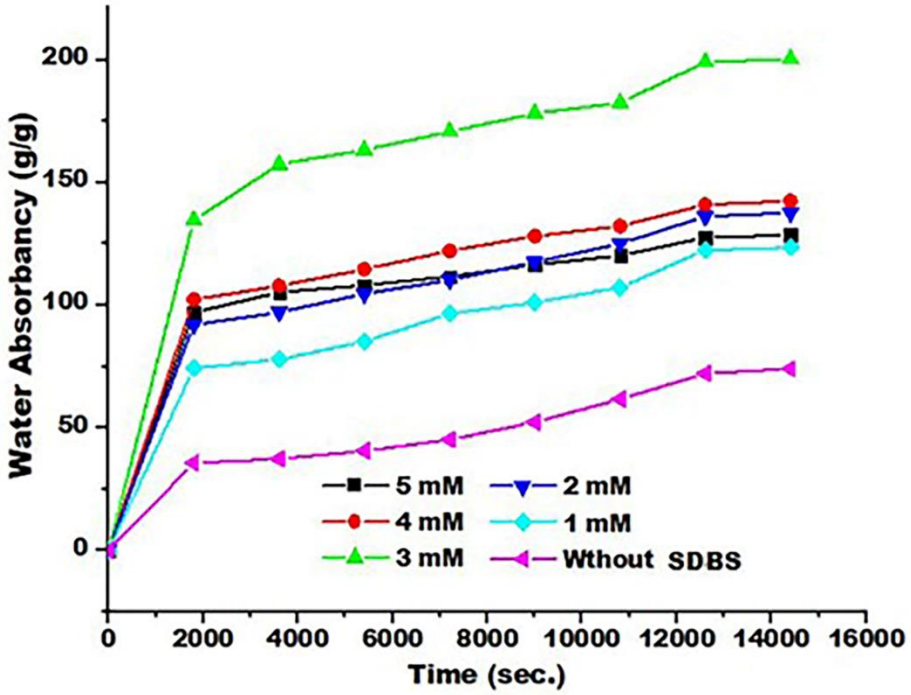

Figure 6. Time-dependent swelling curves of SAPs generated by different concentrations of SDBS in distilled water at pH 7.

3.7. Impact of pH on Water Absorbency and Swelling Kinetics

After selecting SAP6 as the best SAP to absorb distilled water at pH 7, the water absorption capacity of SAP6 was tested at different pHs (2, 4, 9, and 12) at room temperature (Figure 7) and tested at different periods of absorption times (Figure 8). The results showed that the water absorption capacity of the hydrogel increases with increasing pH to 7 and then gradually decreases because the forces of electrostatic repulsion and hydrogen bonding are in equilibrium [46]. The hydrogel's ability to swell or absorb water is low when the pH levels are low due to the strong hydrogen bonding, and the presence of -COOH and NH_2 groups enhances the physical crosslinking in addition to neutralizing the electrostatic repulsion between the –COO- groups, therefore, the prepared SAP network tends to shrink. At the pH range of 4 to 8, ionization of some carboxylic acid groups occurs, as well as electrostatic repulsion between -COO groups, leading to increased swelling of the hydrogel [53].

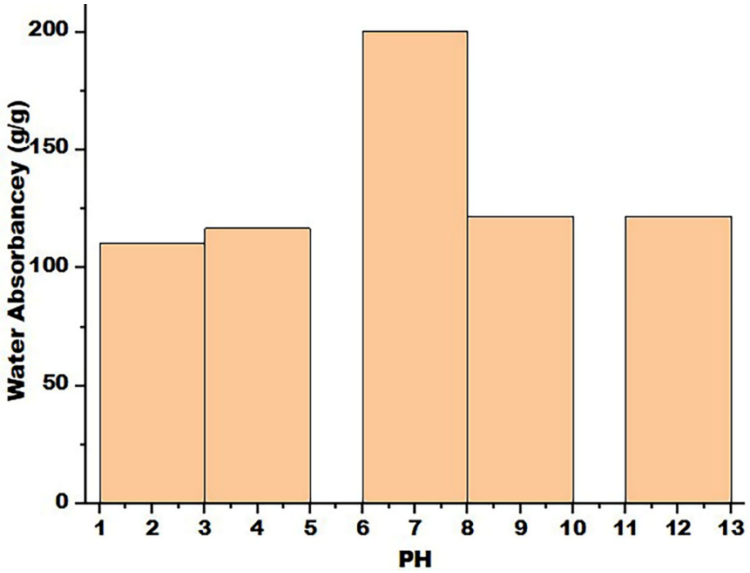

 doi:10.20944/preprints202405.1913.v1

Figure 7. Effect of environmental pH on water absorbency using 3 mM SDBS.

When the pH value is high, the hydrogel swelling ability is low because it is affected by excess sodium ion charges, which protect the carboxylic anions and prevent the formation of an active anion-anion repulsion. The water absorbance capacity increases with increasing pH values until pH 7 and then decreases. In addition, the water absorption capacity increases with increasing immersion time in distaste water until it reaches equilibrium at 12000 to 14000 s at all pH values. Table 5 shows the swelling kinetics parameters such as (K_{it} and S_{∞}) represent a tendency affected by the pH value of the water absorbed by the hydrogel; these parameters increase with increasing pH up to 7 and then decrease gradually. Theoretical equilibrium swelling (S_{∞}) is consistent with the experimental equilibrium swelling (S_{eq}) for all pH values, and the increments of 72% and 82% at pH7 compared with the values of these parameters at pH2. Also, the change in the initial swelling rate constant (K_{it}) is similar to that of the theoretical equilibrium swelling constant and the experimental equilibrium swelling as a function of pH; these results agree with previous studies [54,55].

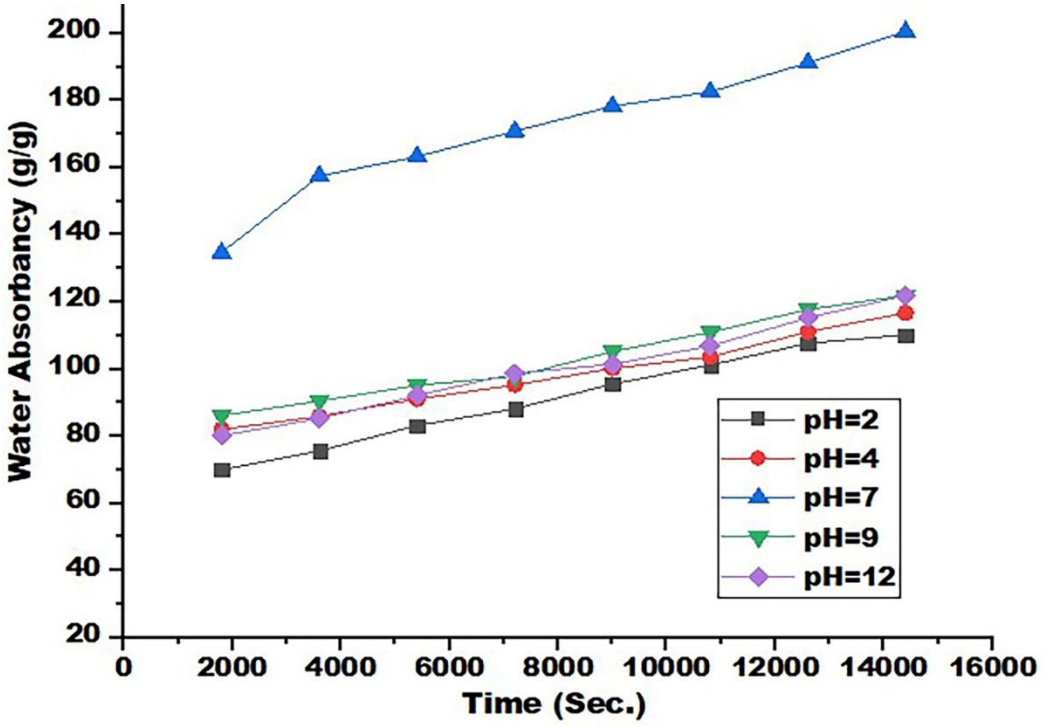

Figure 8. Relation between water absorbency and swelling time for many pH.using 3 mM SDBS.

4. Conclusions

In this work, several superabsorbent polymers (SAPs) were prepared using PUL as a substrate and the grafting polymerization of AA and AM monomers, which is carried out in the presence of a redox pair initiator consisting of KPS/TEMED and MBA using microwave irradiation. FTIR analysis demonstrated that AM/AA grafted onto PUL's macromolecular chains have cross-linking's higher than those of PUL-g-AA or PUL-g- AM. FE-SEM images confirmed that SDBS improves the surface porosity of the hydrogel, which enhances the ability of the hydrogel to absorb large amounts of distilled water. In addition, SDBS improved the grafting parameter and swelling kinetics parameters. Three micromolar concentrations were the best concentration of SDBS, as it has the highest theoretical equilibrium swelling and experimental equilibrium swelling as a function of SDBS and environmental pH.

 doi:10.20944/preprints202405.1913.v1

Authors' Contributions: Corresponding author: Conceptualization, Methodology, Software, Data curation, Writing- Original draft preparation. Auda Jabbar Braihi : Visualization, Investigation, and Supervision Salam Abdulla Dhahir: Software, Validation, Writing- Reviewing and Editing

Acknowledgments: The authors express their sincere thanks and gratitude to all who helped complete this work, especially the employees in the department's laboratories, CAK Company, and Mr. Ali Hussain.

Conflicts of interest: There are no conflicts of interest declared by the author (s).

References

1. S.I. Salih, F.A.Hashem, A.J.Braihi , Preparation and characterization of concrete reinforced by the super-absorbent hydrogel nano composites (SAHNCs) used for construction applications, Adv. nat. appl. sci. 10(2016)112-125.
2. R. Arredondo, Z. Yuan, D. Sosa, A. Johnson, R.F. Beims, H.Li, C.C.Xu, Performance of a novel, eco-friendly, cellulose-based superabsorbent polymer (Cellulo-SAP): Absorbency, stability, reusability, and biodegradability. Can J Chem Eng. 101 (2023)762-1771.
3. A.J. Braihi, S.I.Salih, F.A.Hashem, J.A. Ahmed, Proposed cross-linking model for carboxymethyl cellulose/starch superabsorbent polymer blend. Int. J. Mater. Sci. Eng. 3(2014) 363-369.
4. J. Wei, H. Yang, H. Cao, T. Tan, Using poly aspartic acid hydro-gel as water retaining agent and its effect on plants under drought stress, Saudi J. Biol. Sci., 23 (2016) 654-659.
5. E. Tubert, V.A. Vitali, M.S. Alvarez, F.A. Tubert, I. Baroli, G. Amodeo, Synthesis and evaluation of a superabsorbent-fertilizer composite for maximizing the nutrient and water use efficiency in forestry plantations. J. Environ. Manage. 210 (2018) 239-254.
6. A.Inobeme, A. Ikechukwu Ajai, J. Inobeme, C.O. Adetunji, A. Obar, J.T. Mathew, N. Nwakife, N. , Superabsorbent Polymers for the Development of Nanofiltration. In Properties and Applications of Superabsorbent Polymers: Smart Applications with Smart Polymers (pp. 157-170), Singapore: Springer Nature Singapore, 2023
7. R.A.Rather, M.A.Bhat, A.H. Shalla, An insight into Synthetic, Physiological aspect of Superabsorbent Hydrogels based on Carbohydrate type polymers for various Applications: A Review. Carbohydrate Polymer Technologies and Applications, 100202(2022).
8. X.Shi W. Wang A. Wang , Effect of surfactant on porosity and swelling behaviors of guar gum-poly(sodium acrylate-co-styrene)/attapulgite superabsorbent hydrogels. Colloid Surf B . 88(2011) 279-286.
9. P.A.Mistry, M.N. Konar, S. Latha, U. Chadha, P. Bhardwaj, T.K. Eticha, hitosan Superabsorbent Biopolymers in Sanitary and Hygiene Applications. Int. J. Polym. Sci. 2023(2023).
10. D.Faris, N.J. Hadi, N.J, S.A. Habeeb, Effect of rheological properties of (Poly vinyl alcohol/Dextrin/Naproxen) emulsion on the performance of drug encapsulated nanofibers. Mater. Today Proc. 42(2021) 2725-2732.
11. J.Singh, A. Kumar, A.S. Dhaliwal, Superabsorbent Polymers Application in Agriculture Sector. Properties and Applications of Superabsorbent Polymers: Smart Applications with Smart Polymers, 1st Edition, Springer, 2023.
12. P.R.Sankar, Superabsorbent polymer sponges for the design of saliva absorption pad (Doctoral dissertation, SCTIMST, 2021).
13. A.J. Capezza Villa, Novel superabsorbent materials obtained from plant proteins (2017).
14. X.Shi, W. Wang A. Wang, pH-responsive sodium alginate-based super porous hydrogel generated by an anionic surfactant micelle templating, Carbohyd Polym. 94(2013) 449–455.
15. S.A.Poursamara, M. Azamib, M. Mozafari , Controllable synthesis and characterization of porous polyvinyl alcohol/hydroxyapatite nanocomposite scaffolds via an in situ colloidal technique, Colloid Surf B Biointerfaces 84(2011) 310–316.
16. H.Park, D.Kim, Swelling and mechanical properties of glycol chitosan/poly (vinyl alcohol) IPN-type super porous hydrogels, J Boimed Mater Res Part A. 78 (2006) 662–667.
17. J.T.Delaney, A.R.Liberski, J.Perelaer, U.S.Schubert , Reactive inkjet printing of calcium alginate hydrogel porogen-A new strategy to open-pore structure matrices with controlled geometry, Soft Matter. 6(2010) 866–869
18. D.L.Elbert, Liquid-liquid two-phase systems for the production of porous hydrogels and hydrogel microspheres for biomedical application: a tutorial review, Acta Biomater .7(2011)31–56.
19. S. Partrap, A.Muthutantri, I.U.Rehman, G.R.Davis, J.A.Darr , Preparation and characterization of controlled porosity alginate hydrogels made via a simultaneous micelle templating and internal gelation process, J Mater Sci .42(2007)3502–3507.

20. Shi X, Tangjie, A.Wang , Development of super porous hydroxyethyl cellulose—based hydrogel by anionic surfactant micelle templating with fast swelling and superabsorbent properties. J Appl Polym Sci .132(2015)42027–42034.
21. M.Zhang, S. Zhang, Z. Chen, M. Wang, J. Cao, R. Wang, Preparation and characterization of superabsorbent polymers based on sawdust, Polymers, 11(2019), 1891.
22. Z. Xu, L. Wan, X. Huang, Surface modification by graft polymerization In Surface Engineering of Polymer Membranes, Springer ,2009,
23. S.Chaudhary, V.P. Jain, G. Jaiswar, The composition of polysaccharides: monosaccharides and binding, group decorating, polysaccharides chains. In Innovation in Nano-Polysaccharides for Eco-sustainability (pp. 83-118). Elsevier, 2022
24. S.Rimando, G. Perale, F. Rossi, Polysaccharide-based scaffold for tissue regeneration. In Functional Polysaccharides for Biomedical Applications (pp. 189-212). Woodhead Publishing, 2019
25. S.A. Habeeb, S. A., M.K. Abdulkadhim, Natural Biopolymer-hydrogels Nanofibers for Antibacterial Applications, J Eng Mater Technol. (2023) 1-27.
26. https://doi.org/10.1115/1.4063329
27. Y.Xu, , X. Zhang, X. Zhou, H. Liu, B. Xu, Synergistic interactions between zwitterionic surfactants derived from olive oil and an anionic surfactant, J. Dispers. Sci. Technol.40 (2019) 1308-1316
28. M. Tally, Y. Atassi, Synthesis and characterization of pH-sensitive superabsorbent hydrogels based on sodium alginate-g-poly (acrylic acid-co-acrylamide) obtained via an anionic surfactant micelle templating under microwave irradiation, Polymer Bulletin, 73(2016) 3183–3208.
29. M.Tally, Y. Atassi, Optimized synthesis and swelling properties of a pH-sensitive semi-IPN superabsorbent polymer based on sodium alginate-g-poly (acrylic acid-co-acrylamide) and polyvinylpyrrolidone and obtained via microwave irradiation. J. Polym. Res. 22(2015) 1-13.
30. M. Rizwan, S.R. Gilani, A.I. Durani, S. Naseem, Materials diversity of hydrogel: Synthesis, polymerization process and soil conditioning properties in agricultural field, J. Adv. Res.33(2021) 15-40.
31. A. Mishra, T. Vats, J.H. Clark, Microwave-assisted polymerization. Royal Society of Chemistry (2015). ISBN:978-1-78262-317-5
32. Y.Li, H. Xiao, Y. Pan, M. Zhang, Y. Jin, Thermal and pH dual-responsive cellulose microfilament spheres for dye removal in single and binary systems, J. Hazard. Mater.377(2019) 88-97.
33. T.G.McKenzie, F. Karimi, M. Ashokkumar, G.G. Qiao, Ultrasound and sonochemistry for radical polymerization: sound synthesis, Chem. Eur. J .25(2019) 5372-5388.
34. N.Mohammad, Y. Atassi, M. Tally, Synthesis and swelling behavior of metal-chelating superabsorbent hydrogels based on sodium alginate-g-poly (AMPS-co-AA-co-AM) obtained under microwave irradiation, Polym. Bull. 74(2017) 4453-4481.
35. M.J.Zohuriaan-Mehr, K. Kabiri K, Superabsorbent polymers materials: a review, Iran Polym J 17(2008)451–477.
36. M.El-Sayed, M.Sorour, N. Abd ElMoneem, H.Talaat, H. Shalaan, S. ElMarsafy , Synthesis and properties of natural polymers—grafted-acrylamide. World Appl Sci J .13(2011)360–368
37. H. Ghasemzadeh, F.Ghanaat, Antimicrobial alginate/PVA silver nanocomposite hydrogel, synthesis, and characterization. J Polym Res. 21(2014)355–368
38. S.A.Agnihotri, T.M. Aminabhavi, Novel interpenetrating network chitosan-poly (ethylene oxide-g-acrylamide) hydrogel microspheres for the controlled release of capecitabine, Int. J. Pharm.324(2006) 103-115.
39. Y.Bao, J.Ma, N.Li , Synthesis and swelling behaviors of sodium carboxymethyl cellulose-g-poly(AA-co-AM-co-AMPS)/MMT superabsorbent hydrogel, Carbohydr Polym. 84(2011)76-82
40. B.Sonmez, A.N. Celikkol, Pullulan-based hydrogels for the removal of various metal ions from aqueous solutions, J. Environ. Chem. Eng. 9(2021) 106188.
41. W.M.Mustfa, S.A. Habeeb, Evaluation of the Physical Properties and Filtration Efficiency of PVDF/PAN Nanofiber Membranes by Using Dry Milk Protein, Mater Res Express. (2023). https://doi.org/10.1088/2053-1591/acf6f3
42. F.Ganji, S. Vasheghani-Farahani, E. Vasheghani-Farahani, Theoretical description of hydrogelswelling: a review, Iran Polym J. 19(2010) 375–398
43. J.Wu, F. Zhong, Y. Li, C.F. Shoemaker, W.Xia, , Preparation and characterization of pullulan–chitosan and pullulan–carboxymethyl chitosan blended films, Food Hydrocoll. 30 (2013) 82-91.
44. S.Saber-Samandari, H.O. Gulcan, S. Saber-Samandari, M. Gazi, , Efficient removal of anionic and cationic dyes from an aqueous solution using pullulan-graft-polyacrylamide porous hydrogel, WAT. AIR AND SOIL POLL. 225(2014) 1-14.

 doi:10.20944/preprints202405.1913.v1

45. M.Chen, Z. Ni, Y. Shen, G. Xiang, L. Xu, Reinforced swelling and water-retention properties of super-absorbent hydrogel fabricated by a dual stretchable single network tactic, Colloids Surf. A Physicochem. 602 (2020) 125133.
46. J.Wei, Y. Zhao, S. Yu, J. Du, X. Hu, G. Bai, Z. Wang, Environment-friendly dual-network hydrogel dust suppressant based on xanthan gum, polyvinyl alcohol, and acrylic acid, J. Environ. Manage. 295(2021) 113139.
47. X.Liu, W. Zeng, J. Zhao, X. Qiu, H. Xiong, Y. Liang, X.Ye, Z. Lei, D. Chen, Preparation and anti-leakage properties of hydroxyethyl cellulose-g-poly (butyl acrylate-co-vinyl acetate) emulsion, Carbohydr. Polym.255(2021) 117467.
48. N. Işıklan, G. Küçükbalcı, G., Microwave-induced synthesis of alginate–graft-poly (N-isopropylacrylamide) and drug release properties of dual pH-and temperature-responsive beads, Eur. J. Pharm. Biopharm. 82(2012) 316-331.
49. K. Kabiri ,S. Lashani, M.J.Zouhiriaan-Mehr,M. Kheirabadi M , Superalcohol-absorbent gels of sulfonic acid-contained poly(acrylic acid), J Polym Res .18(2011) 449–458
50. S.M. Khoshkho, , B. Tanhaei, A. Ayati, M. Kazemi, Preparation and characterization of ionic and non-ionic surfactants impregnated κ-carrageenan hydrogel beads for investigation of the adsorptive mechanism of cationic dye to develop for biomedical applications, J. Mol. Liq. 324(2021) 115118.
51. S.G. Warkar, A. Kumar, Synthesis and assessment of carboxymethyl tamarind kernel gum-based novel superabsorbent hydrogels for agricultural applications, Polymer. 182(2019) 121823
52. I.S. Sihama, A.H. Fadhel,A.J. Braihi " Optimization of Nano Graphite Oxide Concentration for Super Absorbent Nano Composites Polymeric Materials" J. Eng. Appl.
53. H. Hosseinzadeh, M. Sadeghzadeh, M. Badazadeh M , Preparation and properties of carrageenan—g-poly (acrylic acid)/bentonite superabsorbent composite. J Boimater Nanobiotechol. 2(2011)311–317
54. M.F.Batouti, W. Sadik, A.G. Eldemerdash, E. Hanafy, H.A. Fetouh, New and innovative microwave-assisted technology for synthesis of guar gum-grafted acrylamide hydrogel superabsorbent for the removal of acid red 8 dye from industrial wastewater, Polym. Bull. 80(2023) 4965-4989.
55. H.Haidari, Z. Kopecki, A.T. Sutton, S. Garg, A.J. Cowin, K. Vasilev, PH-responsive “smart” hydrogel for controlled delivery of silver nanoparticles to infected wounds. Antibiotics, 10(2021) 49
56. F. Jamali, N. Etminani-Esfahani, A. Rahmati, Maleic acid as an important monomer in synthesis of stimuli-responsive poly (acrylic acid-co-acrylamide-co-maleic acid) superabsorbent polymer, Sci Rep. 13(2023) 3511